Excitable Membranes: Channel Noise, Synchronization, and Stochastic Resonance

Peter Hänggi, Gerhard Schmid, and Igor Goychuk

Dept. Physics, University of Augsburg, 86135 Augsburg, Germany

Abstract. By use of a stochastic generalization of the Hodgkin-Huxley model we investigate the phenomena of Stochastic Resonance (SR) and Coherence Resonance (CR) in assemblies of ion channels. If no stimulus is applied we find the existence of an optimal size of the membrane for which the internal noise alone causes a most regular spiking activity (intrinsic CR). In the presence of an applied stimulus we demonstrate SR vs. decreasing patch size (i. e., vs. increasing internal noise strength). SR with external noise occurs only for large sizes which possess sub-optimal internal noise levels. SR in biology thus seemingly is rooted in the collective properties of large ion channel assemblies. Investigating the signal-to-noise ratio (SNR) for sub-threshold sinusoidal driving vs. the frequency we find a bell-shaped behavior vs. frequency which reflects the existence of a random internal limit cycle. Finally we study the role of synchronization vs. decreasing internal noise intensity (i.e. increasing path area).

1 Introduction

A fundamental question in neurophysiology concerns the limiting factors of the reliability of neuronal responses to a given stimulus. In this article we focus on a particular aspect of this complex issue: the impact of *channel noise*, which is generated by the random gating dynamics of the ion channels, on the reliability of signal transmission. In doing so, we consider the effects of stochastic resonance, coherence resonance and synchronization.

During the last decade, the effect of stochastic resonance (SR) – a co-operative phenomenon wherein the addition of external noise improves the detection and transduction of signals in nonlinear systems (for a comprehensive survey and prominent references, see Ref. [1]) – has been studied experimentally and theoretically in various biological systems [2,3,4,5,6]. For example, SR has been experimentally demonstrated within the mechanoreceptive system in crayfish [2], in the cricket cercal sensory system [3], for human tactile sensation [4], visual perception [5], and response behavior of the arterial baroreflex system of humans [6]. The importance of this SR-phenomenon for sensory biology is by now well established; yet, it is presently not known to which minimal level of the biological organization the stochastic resonance effect can ultimately be traced down. Presumably, SR has its origin in the stochastic properties of the ion channel clusters located in a receptor cell membrane. Indeed, for an artificial model system Bezrukov and

Vodyanoy have demonstrated experimentally that a finite ensemble of the alamethicin ion channels does exhibit stochastic resonance [7]. This in turn provokes the question whether a *single* ion channel is able to exhibit SR, or whether stochastic resonance is the result of a *collective* response from a finite assembly of channels.

Stochastic resonance in single, biological potassium ion channels has also been investigated both theoretically [8] and experimentally [9]. This very experiment [9] did not convincingly exhibit SR in single voltage-sensitive ion channels versus the varying temperature. Nevertheless, the SR phenomenon versus the *externally* added noise can occur in single ion channels if only the parameters are within a regime where the channel is predominantly dwelled in the closed state, as demonstrated within a theoretical modeling for a Shaker potassium channel [8]. The manifestation of SR on the *single*-molecular level, is not only of academic interest, but is also relevant for potential nanotechnological applications, such as the design of single-molecular biosensors. The origin and biological relevance of SR in single ion channels, however, remains still open.

Indeed, biological SR can be a manifestation of *collective* properties of large assemblies of ion channels of different sorts. To display the phenomenon of excitability these assemblies must contain an assemblage of ion channels of at least two different sorts – such as, *e.g.*, potassium and sodium channels. The corresponding mean-field type model has been put forward by Hodgkin and Huxley in 1952 [10] by neglecting the mesoscopic fluctuations which originate from the stochastic opening and closing of channels. SR due to *external* noise in this primary model and related models of excitable dynamics has extensively been addressed [11]. These models further display another interesting effect in the presence of noise, namely so termed coherence resonance (CR) [12,13]: even in absence of an external periodic signal the stochastic dynamics exhibits a surprisingly more regular behavior due to an optimally applied external noise intensity.

Synchronization presents another phenomenon, which is also closely related to SR and CR [14,15]. The mechanisms of synchronization are presently well-established for some chaotic and excitable systems. Depending on the type and strength of coupling, several kinds of synchronization can be distinguished: complete synchronization, generalized synchronization, lag synchronization, phase synchronization, and burst (or train) synchronization [14,15]. In the context of excitable systems, frequency and phase synchronization has been found, for example, in the integrate-and-fire model of neuron driven by white noise and an externally applied stochastic spike train [16]. Namely, for an optimal dose of noise the mean firing rate of the driven neuron becomes locked by the mean frequency of the external spike train [16].

A challenge though still remains: does *internal* noise play a constructive role for SR, CR and synchronization? Internal noise is produced by fluctuation of the number of open channels within the assembly, and diminishes

with increasing number of channels. For a large, macroscopic number of channels this noise becomes negligible. Under the realistic biological conditions, however, it may play an important role [17].

2 The Hodgkin-Huxley Model

Our starting point is due to the model of Hodgkin and Huxley [10], *i.e.* the ion current across the biological membrane is carried mainly by the motion of sodium, Na^+, and potassium, K^+, ions through the selective and voltage-gated ion channels embedded across the membrane. Besides, there is also a leakage current present which is induced by chloride and remaining other ions. The ion channels are formed by special membrane proteins which undergo spontaneous, but voltage-sensitive conformational transitions between open and closed states [18]. Moreover, the conductance of the membrane is directly proportional to the number of the *open* ion channels. This number depends on the potential difference across the membrane, V. The different concentrations of the ions inside and outside the cell are encoded by corresponding reversal potentials $E_{Na} = 50$ mV, $E_K = -77$ mV and $E_L = -54.4$ mV, respectively, which give the voltage values at which the direction of partial ion currents is reversed [18]. Taking into account that the membrane possesses a capacitance $C = 1\ \mu\mathrm{F/cm^2}$, Kirchhoff's first law reads in presence of an *external* current $I_{ext}(t)$ stimulus:

$$C\frac{d}{dt}V + G_K(n)\ (V - E_K) + G_{Na}(m,h)\ (V - E_{Na}) + G_L\ (V - E_L) = I_{ext}(t)\,. \quad (1)$$

Here, $G_{Na}(m,h)$, $G_K(n)$ and G_L denote the conductances of sodium, potassium, and the remaining other ion channels, respectively. The leakage conductance is assumed to be constant, $G_L = 0.3\mathrm{mS/cm^2}$; in contrast, those of sodium and potassium depend on the probability to find the ion channels in their open conformation. To explain the experimental data, Hodgkin and Huxley did assume that the conductance of a potassium channel is gated by four independent and identical gates. Thus, if n is the probability of one gate to be open, the probability of the K^+ channel to stay open is $P_K = n^4$. Moreover, the gating dynamics of sodium channel is assumed to be governed by three independent, identical gates with opening probability m and an additional one, being different, possessing the opening probability h. Accordingly, the opening probability of Na^+ channel (or the fraction of open channels) reads $P_{Na} = m^3h$. The conductances for potassium and sodium thus read

$$G_K(n) = g_K^{\max}\, n^4, \quad G_{Na}(m,h) = g_{Na}^{\max}\, m^3 h\,, \quad (2)$$

where $g_{\mathrm{Na}}^{\max} = 120$ mS/cm^2 and $g_{\mathrm{K}}^{\max} = 36$ mS/cm^2 are the maximal conductances. Furthermore, the gating variables (probabilities) m, h and n obey the two-state, "opening-closing" dynamics,

$$\begin{aligned} \dot{m} &= \alpha_m(V)\ (1-m) - \beta_m(V)\ m\,, \\ \dot{h} &= \alpha_h(V)\ (1-h) - \beta_h(V)\ h\,, \\ \dot{n} &= \alpha_n(V)\ (1-n) - \beta_n(V)\ n\,, \end{aligned} \tag{3}$$

with the experimentally determined voltage-dependent transition rates, reading for a squid giant axon [10,19]:

$$\alpha_m(V) = \frac{0.1(V+40)}{1-\exp[-(V+40)/10]}\,,$$

$$\beta_m(V) = 4\ \exp[-(V+65)/18]\,, \tag{4a}$$

$$\alpha_h(V) = 0.07\ \exp[-(V+65)/20]\,,$$

$$\beta_h(V) = \{1+\exp[-(V+35)/10]\}^{-1}\,, \tag{4b}$$

$$\alpha_n(V) = \frac{0.01\ (V+55)}{1-\exp[-(V+55)/10]}\,,$$

$$\beta_n(V) = 0.125\ \exp[-(V+65)/80]\,. \tag{4c}$$

The rate constants in (4a)–(4c) are given in ms^{-1} and the voltage in mV. These nonlinear Hodgkin-Huxley equations (1)–(4c) present a cornerstone model in neurophysiology. Within the same line of reasoning this model can be generalized to a mixture of different ion channels with various gating properties [19,20].

3 Stochastic Version of the Hodgkin-Huxley Model

It has been suspected since the time of Hodgkin and Huxley, and known with certainty since the first single-channel recordings of Neher, Sakmann and colleagues, that voltage-gated ion channels are stochastic devices [21]. An essential drawback of the Hodgkin-Huxley model, however, is that it operates with the *average* number of open channels, thereby disregarding the corresponding number fluctuations (or, the so-called *channel noise* [21,17]). These fluctuations, i.e. their strength, scale inversely proportional to the number of ion channels, see eq. (6) below. Thus, the original Hodgkin-Huxley model can be valid, strictly speaking, only within the limit of very large system size. We emphasize, however, that the size of an excitable membrane patch within a neuron is typically finite. As a consequence, the role of internal fluctuations cannot be *a priori* neglected [17]. As a matter of fact, as shown below, they do play a key role for SR, CR, and synchronization.

3.1 Quantifying Channel Noise

The role of channel noise for the neuron firing has been first studied by Lecar and Nossal as early as in 1971 [22]. The corresponding stochastic generaliza-

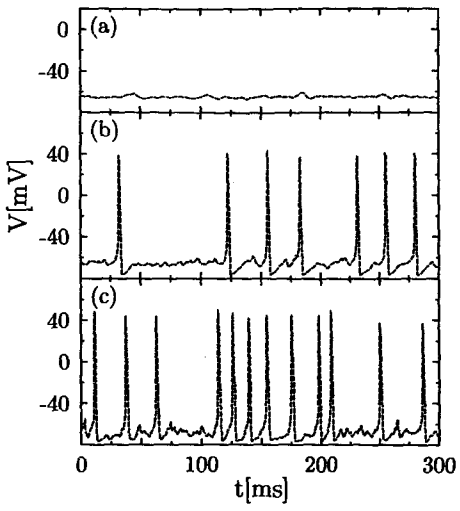

Fig. 1. Numerical simulation of the stochastic Hodgkin-Huxley system (1),(5),(6) with vanishing external stimulus. We computed several realizations of the voltage signal for different numbers of the ion channels: a) $N_{Na} = 6000$, $N_K = 1800$; b) $N_{Na} = 600$, $N_K = 180$; and c) $N_{Na} = 60$, $N_K = 18$. Upon decreasing the system size the influence of channel noise on the spontaneous firing dynamics becomes more and more pronounced. Note that the non-stochastic Hodgkin-Huxley model does not exhibit spikes at all for the parameters given in the text and in the absence of external stimuli

tions of Hodgkin-Huxley model (within a kinetic model which corresponds to the above given description) has been put forward by DeFelice *et al.* [23] and others; see [17] for a review and further references therein. The main conclusion of these previous studies is that the channel noise can be functionally important for neuron dynamics. In particular, it has been demonstrated that channel noise alone can give rise to a spiking activity even in the absence of any stimulus [17,23,24].

To include the channel noise influence in a theoretical modeling within the stochastic kinetic schemes [17,23], however, necessitates extensive numerical simulations [25]. To aim at a less cumbersome numerical scheme we use a short-cut procedure that starts from Eq. (3) in order to derive a corresponding set of Langevin equations for a stochastic generalization of the Hodgkin-Huxley equations of the type put forward by Fox and Lu [26]. Following their reasoning we substitute the equations (3) with the corresponding Langevin generalization:

$$\begin{aligned} \dot{m} &= \alpha_m(V)\ (1-m) - \beta_m(V)\ m + \xi_m(t)\,, \\ \dot{h} &= \alpha_h(V)\ (1-h) - \beta_h(V)\ h + \xi_h(t)\,, \\ \dot{n} &= \alpha_n(V)\ (1-n) - \beta_n(V)\ n + \xi_n(t)\,, \end{aligned} \tag{5}$$

with independent Gaussian white noise sources of vanishing mean. The noise autocorrelation functions depend on the stochastic voltage and the corre-

sponding total number of ion channels as follows

$$\begin{aligned}
\langle \xi_m(t)\xi_m(t')\rangle &= \frac{2}{N_{\mathrm{Na}}}\,\frac{\alpha_m\beta_m}{(\alpha_m+\beta_m)}\,\delta(t-t')\,,\\
\langle \xi_h(t)\xi_h(t')\rangle &= \frac{2}{N_{\mathrm{Na}}}\,\frac{\alpha_h\beta_h}{(\alpha_h+\beta_h)}\,\delta(t-t')\,,\\
\langle \xi_n(t)\xi_n(t')\rangle &= \frac{2}{N_{\mathrm{K}}}\,\frac{\alpha_n\beta_n}{(\alpha_n+\beta_n)}\,\delta(t-t')\,.
\end{aligned} \tag{6}$$

In order to confine the conductances between the physically allowed values between 0 (all channels are closed) and $g^{\max}$ (all channels are open) we have implemented numerically the constraint of reflecting boundaries so that $m(t)$, $h(t)$ and $n(t)$ are always located between zero and one [26].

Moreover, the numbers N_{Na} and N_{K} depend on the actual area S of the membrane patch. With the assumption of homogeneous ion channel densities, $\rho_{\mathrm{Na}} = 60\ \mu\mathrm{m}^{-2}$ and $\rho_{\mathrm{K}} = 18\ \mu\mathrm{m}^{-2}$, one finds the following scaling behavior

$$N_{\mathrm{Na}} = \rho_{\mathrm{Na}} S, \quad N_{\mathrm{K}} = \rho_{\mathrm{K}} S\,. \tag{7}$$

Upon decreasing the system size S, the fluctuations and, hence, the internal noise increases. Consequently, with abating cell membrane patch the spiking behavior changes dramatically, cf. Fig. 1.

3.2 Numerical Integration

Before integrating the system of stochastic equations (1), (5), (6) numerically, the external stimulus $I_{\mathrm{ext}}(t)$ must be specified. We take a periodic stimulus of the form

$$I_{\mathrm{ext}}(t) = A\ \sin(\Omega t) + \eta(t)\,, \tag{8}$$

where the sinusoidal signal with amplitude A and angular frequency Ω is contaminated by the Gaussian white noise $\eta(t)$ with the autocorrelation function

$$\langle \eta(t)\eta(t')\rangle = 2D_{\mathrm{ext}}\ \delta(t-t')\,, \tag{9}$$

and noise strength D_{ext}.

The numerical integration is carried out by the standard Euler algorithm with the step size $\Delta t \approx 2\cdot 10^{-3}$ ms. The "Numerical Recipes" routine `ran2` is used for the generation of independent random numbers [27] with the Box-Muller algorithm providing the Gaussian distributed random numbers. The total integration time is chosen to be a multiple of the driving period $T_\Omega = 2\pi/\Omega$, as to ensure that the spectral line of the driving signal is centered on a computed value of the power spectral densities. From the stochastic voltage signal $V(t)$ we extract a point process of spike occurrences $\{t_i\}$:

$$u(t) := \sum_{i=1}^{N} \delta(t-t_i)\,, \tag{10}$$

where N is the total number of spikes occurring during the elapsed time interval. The occurrence of a spike in the voltage signal $V(t)$ is obtained by upward-crossing a certain detection threshold value V_0. It turns out that the threshold can be varied over a wide range with no effect on the resulting spike train dynamics. The power spectral density of the spike train (PSD_u), the interspike interval histogram (ISIH) and the coefficient of variation (CV) have been analyzed. The coefficient of variation CV, which presents a measure of the spike coherence, reads:

$$\mathrm{CV} := \frac{\sqrt{\langle T^2\rangle - \langle T\rangle^2}}{\langle T\rangle}, \tag{11}$$

where $\langle T\rangle := \lim_{N\to\infty} \sum(t_{i+1}-t_i)/N$ and $\langle T^2\rangle := \lim_{N\to\infty} \sum(t_{i+1}-t_i)^2/N$ are the mean and mean-squared interspike intervals, respectively. From the PSD_u we obtain the height of the spectral line of the periodic stimulus as the difference between the peak value and its background offset. The signal-to-noise ratio (SNR) is then given by the ratio of signal peak height to the background height (in the units of spectral resolution of signals).

3.3 Coherence Resonance and Synchronization

We have analyzed the spike coherence in the autonomous, nondriven regime (*i.e.*, we have used $I_{\mathrm{ext}} = 0$) as a function of the decreasing cluster size. Our simulation reveals, cf. Fig. 2(a), the novel phenomenon of *intrinsic coherence resonance*, where the order in the spike sequence increases; *i.e.* the CV is falling, *solely due to the presence of internal noise.* The fully disordered

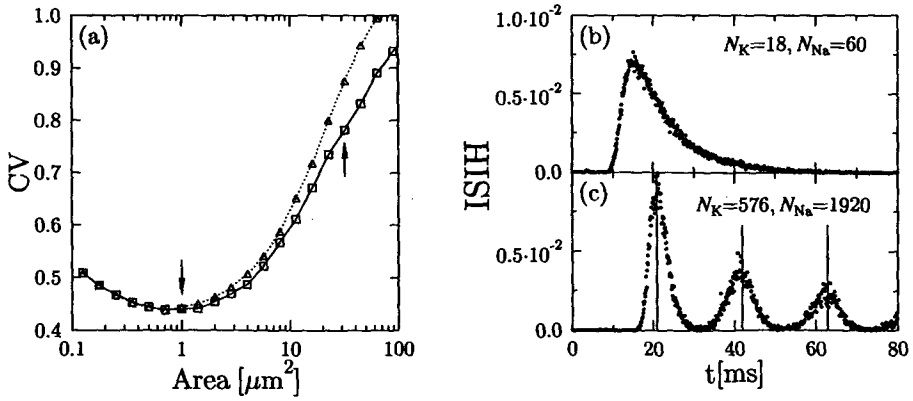

Fig. 2. (a) The coefficient of variation (CV) in (11) is plotted versus the area S in absence of external noise $D_{\mathrm{ext}} = 0$ for periodic sub-threshold driving with $A = 1.0$ $\mu\mathrm{A/cm}^2$ and $\Omega = 0.3$ ms^{-1} (solid line) and without any stimulus (dotted line). The ISIH are depicted in the presence of the periodic signal for $S = 1$ $\mu\mathrm{m}^2$ (b), see downward arrow in (a), and $S = 32$ $\mu\mathrm{m}^2$ (c), see upward arrow in (a). The vertical lines denote the driving period and its first two multiples

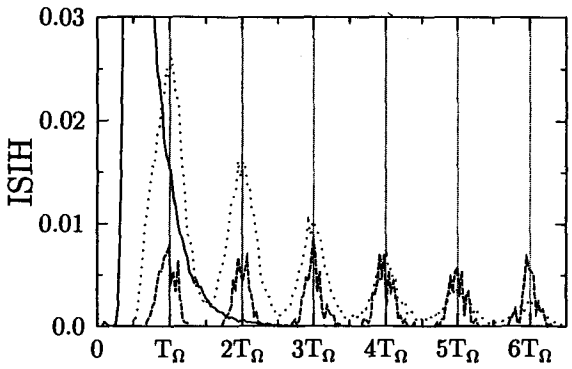

Fig. 3. The interspike interval histogram is plotted for the external stimulus $I_{\text{ext}}(t) = \sin(0.2 \cdot t)$ [μA/cm^2] and different observation areas: $S = 1$ μm^2 (solid line), $S = 32$ μm^2 (dotted line), and $S = 128$ μm^2 (dashed line). For not too small patch sizes the spike occurrences synchronize with the external sinusoidal stimulus at multiples of the driving frequency T_Ω

sequence (which corresponds to a Poissonian spike train) would assume the value CV = 1. We note, however, that near $S = 1$ μm^2 (optimal dose of internal noise), CV ≈ 0.44, *i.e.* the spike train becomes distinctly more ordered! For $S < 1$ μm^2, the internal noise increases further beyond the optimal value and destroys the order in spiking again. It is worth noting that for $S < 1$ μm^2 the model reaches limiting validity; in that regime the kinetic scheme [17,23,24,25] should be used instead. Such a corresponding study, however, has been put forward independently by Jung and Shuai [25]; their results are in qualitative agreement with our findings.

Next we switch on an external sub-threshold sinusoidal driving. Interestingly enough the interspike intervals distribution is not affected for small patch sizes, cf. Fig. 2(b). In this case, the spike-activity possesses an internal rhythm which dominates over the external disturbances. For larger patch sizes the internal noise decreases and the periodic drive induces a reduction of the CV as compared to the undriven case, note the right arrow in Fig. 2(a). In this latter regime the external driving rules the spiking activity as depicted with the characteristic peaks in the ISIH in Fig. 2(c) at multiple driving periods.

In the deterministic limit the Hodgkin-Huxley equations exhibit the phenomenon refractoriness, i.e. no firing event occurs before a minimal time interval of about 15 ms has elapsed since the last firing [10]. In the presence of channel noise, see Fig. 1, the refractory time interval (or dead-time) becomes reduced [24,25]; note the distinct reduction of 12–13 ms in Fig. 2(b) and (c).

For a different sub-threshold driving, with the amplitude $A = 1$ μA/cm^2 and frequency $\Omega = 0.2$ ms^{-1}, the ISIH is plotted for different patch areas in Fig. 3. In the intermediate and small noise regime the spike occurrences are locked to the multiples of driving period. Even though such locking presents clearly a synchronization behavior, the perfect frequency synchronization, characterized by the Rice frequency $\langle\omega\rangle := \lim_{N\to\infty} 2\pi/N \sum_{i=1}^{N} 1/(t_{i+1} - t_i)$, could not be detected. In fact, a frequency mismatch between the driving

frequency Ω and the Rice frequency $\langle\omega\rangle$ has been observed (not shown). This frequency mismatch happens due to the multimodal structure of the ISIH, which is caused by the locking of firing occurrences to the external force period in ratios different from 1:1. A similar phenomenon of imperfect synchronization has also been found in human cardiorespiratory activity [28].

3.4 Stochastic Resonance

Next, the focus is on the SNR in absence of external noise, see Fig. 4(a). Here we discover the novel effect of genuine *intrinsic stochastic resonance*, where the response of the system to the sub-threshold external stimulus is optimized *solely* due to internal, ubiquitous noise. For the given parameters it occurs at $S \approx 32\ \mu m^2$. For $S < 32\ \mu m^2$ growing internal noise monotonically deteriorates the system response. Under such circumstances, one would predict that the addition of an external noise (which corresponds to the conventional situation in biological SR studies) *cannot* improve SNR further, *i.e.* conventional SR will not be exhibited. Our numerical simulations, Fig. 4(b), fully confirm this prediction. Conventional stochastic resonance therefore occurs only for large membrane patches beyond optimal size, and reaches saturation in the limit $S \to \infty$ (limit of the deterministic Hodgkin-Huxley model). Thus, the observed biological SR [2,3] is rooted in the collective properties of large ion channels arrays, where ion channels are globally coupled via the common membrane potential $V(t)$.

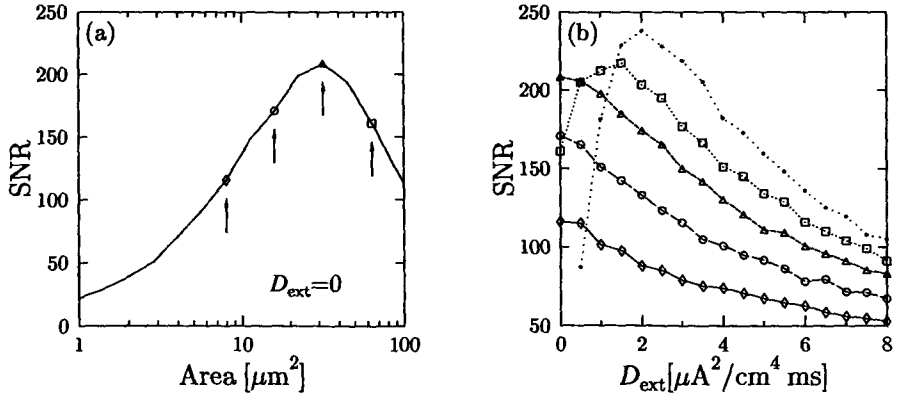

Fig. 4. The signal-to-noise ratio (SNR) for an external sinusoidal stimulus with amplitude $A = 1.0\ \mu A/cm^2$ and angular frequency $\Omega = 0.3\ ms^{-1}$ for different observation areas: (a) no external noise is applied; (b) SNR versus the external noise for the system sizes indicated by the arrows in Fig. 4(a): $S = 8\ \mu m^2$, solid line through the diamonds; $S = 16\ \mu m^2$, long dashed line connecting the circles; $S = 32\ \mu m^2$, short dashed line through the triangles; $S = 64\ \mu m^2$, dotted line connecting the squares. The situation with no internal noise (*i.e.*, formally $S \to \infty$) is depicted by the dotted line connecting the filled dots

In addition, by changing the driving frequency we rediscover the effect of combined stochastic and conventional resonance [13], cf. Fig. 5. In other words, SNR becomes optimized not only versus the patch size, but also versus the driving frequency. Moreover, due to the noisy character of gating variables, the mean frequency of a corresponding random limit cycle in the stochastic Hodgkin-Huxley model (1),(5),(6) depends on the membrane patch area. Thus, the maxima of SNR are located for various system sizes at different driving frequencies.

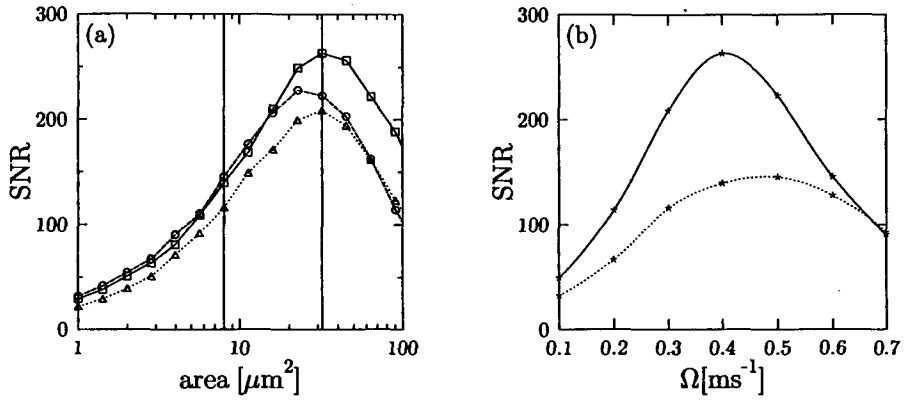

Fig. 5. The signal-to-noise ratio (SNR) for a sub-threshold external stimulus with amplitude $A = 1.0$ $\mu A/cm^2$ and different angular frequencies: (a) SNR versus the observation area for $\Omega = 0.3$ ms^{-1} (dotted line through the triangles), $\Omega = 0.4$ ms^{-1} (solid line connecting the squares), and $\Omega = 0.5$ ms^{-1} (dashed line through the circles); (b) SNR versus the driving frequency for two areas ($S = 8$ μm^2, dotted line; $S = 32$ μm^2, solid line), depicted by vertical lines in Fig. 5(a). The curves exhibit clear maxima and, therefore, the effect of double-stochastic resonance

4 Conclusions

In conclusion, we have investigated the stochastic resonance and the coherence resonance [24], as well as the synchronization in a noisy generalization of the Hodgkin-Huxley model. The spontaneous fluctuations of the membrane conductivity due to the individual ion channel dynamics has systematically been taken into account. We have shown that the excitable membrane patches with observation area around $S \approx 1$ μm^2 exhibit a rhythmic spiking activity optimized by omnipresent internal noise. In other words, the collective dynamics of globally coupled ion channels become more ordered solely due to *internal* noise. This new effect can be regarded as the *intrinsic coherence resonance* phenomenon; it presents a first important result of our work. This very finding has also been confirmed independently within a complementary approach by Jung and Shuai [25]. Moreover, for the case of a sub-threshold

periodic driving we have shown that for intermediate patch sizes a synchronization of firing events with the multiplies of the driving period occurs. This is reflected by an improper synchronization between the Rice frequency and the frequency of external driving.

The second main result of this study refers to the phenomenon of *intrinsic SR*. Here, the channel noise *alone* gives rise to SR behavior, cf. Fig. 4(a) (see also Ref. [25]). Moreover, such intrinsic SR is optimized versus the driving frequency, cf. Fig. 5. Conventional SR versus the external noise intensity also takes place, but for sufficiently large membrane patches, where the internal noise strength alone is not yet at its optimal value. We thus conclude that the observed biological SR likely is rooted in the *collective* properties of globally coupled ion channel assemblies.

The authors gratefully acknowledge the support of this work by the Deutsche Forschungsgemeischaft, SFB 486 *Manipulation of matter on the nanoscale*, project A10. Moreover, we appreciate most helpful and constructive discussions with Peter Jung and Alexander Neiman.

References

1. L. Gammaitoni, P. Hänggi, P. Jung, and F. Marchesoni, Rev. Mod. Phys. **70**, 223 (1998).
2. J.K. Douglass, L. Wilkens, E. Pantazelou, and F. Moss, Nature (London) **365**, 337 (1993).
3. J.E. Levin, and J.P. Miller, Nature (London) **380**, 165 (1996).
4. J.J. Collins, T.T. Imhoff, and P. Grigg, Nature (London) **383**, 770 (1996).
5. E. Simonotto, M. Riani, C. Seife, M. Roberts, J. Twitty, and F. Moss, Phys. Rev. Lett. **78**, 1186 (1997).
6. I. Hidaka, D. Nozaki, and Y. Yamamoto, Phys. Rev. Lett. **85**, 3740 (2000).
7. S.M. Bezrukov, and I. Vodyanoy, Nature (London) **378**, 362-364 (1995); **385**, 319 (1997).
8. I. Goychuk, and P. Hänggi, Phys. Rev. E **61**, 4272 (2000).
9. D. Petracchi, M. Pellegrini, M. Pellegrino, M. Barbi, and F. Moss, Biophys. J. **66**, 1844 (1994).
10. A.L. Hodgkin, and A.F. Huxley, J. Physiol. (London) **117**, 500 (1952).
11. A. Longtin, J. Stat. Phys. **70**, 309-327(1993); K. Wiesenfeld, D. Pierson, E. Pantazelou, C. Dames, and F. Moss, Phys. Rev. Lett. **72**, 2125 (1994); J.J. Collins, C.C. Chow, A.C. Capela, and T.T. Imhoff, Phys. Rev. E **54**, 5575 (1996); S.-G. Lee, and S. Kim, Phys. Rev. E **60**, 826 (1999).
12. A.S. Pikovsky, and J. Kurths, Phys. Rev. Lett. **78**, 775 (1997); S.-G. Lee, A. Neiman, and S. Kim, Phys. Rev. E **57**, 3292 (1998).
13. B. Lindner, and L. Schimansky-Geier, Phys. Rev. E **61**, 6103 (2000).
14. A. Pikovsky, M. Rosenblum, and J. Kurths, *Synchronization: A Universal Concept in Nonliear Sciences* (Cambridge University Press, Cambridge 2001).
15. Y. Kuramoto, *Chemical Oscillations, Waves and Turbulence* (Springer, Berlin, 1984).
16. A. Neiman, L. Schimansky-Geier, F. Moss, B. Shulgin, and J.J. Collins, Phys. Rev. E **60**, 284 (1999).

17. J.A. White, J.T. Rubinstein, and A.R. Kay, Trends Neurosci. **23**, 131 (2000).
18. B. Hille, *Ionic Channels of Excitable Membranes*, 2nd ed. (Sinauer Associates, Sunderland, MA 1992).
19. R.J. Nossal, and H. Lecar, *Molecular and Cell Biophysics* (Addison-Wesley, Redwood City 1991).
20. S.B. Lowen, L.S. Liebovitch, and J.A. White, Phys. Rev. E **59**, 5970 (1999).
21. B. Sakmann, and E. Neher, *Single-Channel recording* (Plenum Press, 1995).
22. H. Lecar, and R. Nossal, Biophys. J. **11**, 1068 (1971).
23. J.R. Clay, and L.J. DeFelice, Biophys. J. **42**, 151 (1983); A.F. Strassberg, and L.J. DeFelice, Neural Comput. **5**, 843 (1993); L.J. DeFelice, and A. Isaac: Chaotic states in a random world, J. Stat. Phys. **70**, 339 (1993).
24. G. Schmid, and I. Goychuk, P. Hänggi, Europhys. Lett. **56**, 22 (2001).
25. P. Jung, and J. W. Shuai, Europhys. Lett. **56**, 29 (2001).
26. R.F. Fox R, and Y. Lu, Phys. Rev. E **49**, 3421 (1994).
27. W.H. Press, S.A. Teukolsky, W.T. Vetterling, and B.P. Flannery, *Numerical Recipes in C*, 2nd ed. (Cambridge Univ. Press, Cambridge 1992).
28. C. Schäfer, M.G. Rosenblum, J. Kurths, and H.-H. Abel, Nature (London) **392**, 239 (1998); C. Schäfer, M.G. Rosenblum, H.-H. Abel, and J. Kurths, Phys. Rev. E **60**, 857 (1999).